Nonlinear Optical Materials | Hot Paper

How to cite:
International Edition: doi.org/10.1002/anie.202202096
German Edition: doi.org/10.1002/ange.202202096

Strong Nonlinearity Induced by Coaxial Alignment of Polar Chain and Dense [BO_3] Units in $CaZn_2(BO_3)_2$

Miriding Mutailipu, Fuming Li, Congcong Jin, Zhihua Yang, Kenneth R. Poeppelmeier, and Shilie Pan**

Abstract: Discovery of new efficient nonlinear optical (NLO) materials with large second-order nonlinearity for the short-wave ultraviolet spectral region ($\lambda_{PM} \leq$ 266 nm, PM = phase-matching) is still very challenging. Herein, a new beryllium-free borate $CaZn_2(BO_3)_2$ with $Sr_2Be_2B_2O_7$ (SBBO) double-layered like configuration was rationally designed, which not only preserves the structural merits but also eliminates the limitations of the SBBO crystal. $CaZn_2(BO_3)_2$ shows a large PM second harmonic generation (SHG) reponse of 3.8× KDP, which is 38 times higher than that of its barium analogue. This enhancement mainly originates from the $^1[Zn_2O_6]_\infty$ polar chains with a large net dipole moment and [BO_3] units with a high NLO active density. Our findings show the great significance of the [ZnO_4] tetrahedra introduced strategy to design beryllium-free SBBO-type NLO crystals and also verify the feasibility of using simple non-isomorphic substitution to induce giant second-order nonlinearity enhancement.

Nonlinear optical (NLO) crystals, especially those that can realize the fourth (266 nm) and sixth (177.3 nm) harmonic generation from the most common 1064 nm laser source, are versatile materials, and thus an ever-growing emphasis is being placed on functionalizing these crystals into optical devices for laser-driven applications.[1] Second-order nonlinearity is the foremost parameter and can be expressed as second-order susceptibility tensor $\chi^{(2)}$, depending on the hyperpolarizability of the microscopic unit and its arrangement in the lattice.[2] And also, as the second-order susceptibility tensor $\chi^{(2)}$ is non-zero for compounds that lack inversion symmetry, the second-harmonic field can only occur with crystals in certain non-centrosymmetric classes.[3] Thus, non-centrosymmetric packing of atoms or molecular units is the prerequisite for designing crystalline materials showing second-order nonlinearities. These NLO-active units should be in favorable arrangements to induce the local distortions for a large nonlinearity.[4] In principle, a large nonlinearity is beneficial for achieving high power and efficiency during the frequency doubling conversion process.[1d] Thus, an important target for NLO materials research is the discovery of such candidates that display high second-order nonlinearities or achievement of large enhancement.

In order to discover crystals with large second-order nonlinearities, the NLO active units used mainly include: i) π-conjugated units,[4b,5] ii) non-π-conjugated tetrahedra;[6] iii) polar-chalcogenide tetrahedra,[4d,7] iv) distorted polyhedra with d^0 or d^{10} cations,[8] and v) lone pair cations with stereoactivity.[4a,c,9] The introduction of these units is beneficial for the local formation of dipolar moments in the lattice. However, the association of NLO units in a non-centrosymmetric framework in optimally aligned configurations is not straightforward. In fact, especially for inorganic crystals, the homogeneity of bond strengths does not allow to single-out a specific group of NLO active units and hence to state that their use can guarantee crystals with large enough second-order nonlinearities. Thus, many NLO crystals with weak second-order nonlinearities consisting of the five type units listed previously are often found as the NLO active units are in unfavorable arrangements.

The realization of significant large nonlinearities enhancement can be realized by increasing the microscopic hyperpolarizability and density of NLO active units and arranging in the same-direction since their contributions fully add to the total nonlinearity, which observed strongly depends on multifarious chemical modifications exemplified by reported NLO crystals over recent years.[8b,c,e,f,9d] Among them, substitution or co-substitution based on the classic structural framework is the simplest effective strategy. For example, the nonlinear coefficient (d_{36}) of $NH_4H_2PO_4$ is about twice as large as that of its isomorphic KH_2PO_4 crystal, which can be attributed to the roles of hydrogen bonds when replacing K^+ with NH_4^+ cations.[10] Owing to the Pb-chelated [BO_3] groups configuration and cation coordination control, $Pb_2Ba_3(BO_3)_3Cl$ and $BaZn(BO_3)F$ exhibit about six times larger nonlinearities compared to $Ba_5(BO_3)_3Cl$ and $BaMg(BO_3)F$.[9c,11] Although there is a considerable nonlinearity enhancement in these examples,

[*] Prof. M. Mutailipu, F. Li, C. Jin, Prof. Z. Yang, Prof. S. Pan
CAS Key Laboratory of Functional Materials and Devices for Special Environments, Xinjiang Key Laboratory of Electronic Information Materials and Devices, Xinjiang Technical Institute of Physics & Chemistry, CAS, 40-1 South Beijing Road, Urumqi 830011 (China)
and
Center of Materials Science and Optoelectronics Engineering, University of Chinese Academy of Sciences
Beijing 100049 (China)
E-mail: slpan@ms.xjb.ac.cn

Prof. K. R. Poeppelmeier
Department of Chemistry, Northwestern University
2145 Sheridan Road, Evanston, IL 60208–3113 (USA)
E-mail: krp@northwestern.edu

the significant improvement (>10 times) remains difficult to achieve, especially for deep-UV transparent NLO crystals.

Some classic crystals have novel structural frameworks that can induce good optical properties, such as the layered configuration of $KBe_2BO_3F_2$ (KBBF) and $Sr_2Be_2B_2O_7$ (SBBO),[12] structural optimization based on them has been well documented. One of the main ideas is to replace $[BeO_4]$/$[BeO_3F]$ with similar $[TO_{4-n}X_n]$ ($n=1$–3) tetrahedra, where strongly covalent T atoms such as Al, Zn, and B are most commonly used.[6b,8b–d,13] For example, the substitution of Be-based tetrahedra with $[ZnO_3X]$/$[ZnO_4]$ components based on the KBBF crystal led to the discovery of several new borates, like $AZn_2BO_3X_2$ (A = ammonium or alkali metal; X = halogen),[8b–d] and $BaZnM_2(BO_3)_2F_2$ (M = Zn and Be), etc.[14] However, there are still no SBBO-type NLO borates reported following the strategy of $[BeO_4]$-$[ZnO_4]$ tetrahedra substitution. In this Communication, the first NLO zinc borate with an SBBO-type structure, $CaZn_2(BO_3)_2$ (CZBO), which shows a large phase-matching (PM) SHG reponse of 3.8×KDP and that is 38 times higher than that of its non-isomorphic $BaZn_2(BO_3)_2$ parent is reported. The origin of such a large enhancement was confirmed and modelled by several different approaches.

CZBO crystallizes in the non-centrosymmetric space group of *Aba*2 (Table S1, detailed crystal data is also available in ref. [15]), which is not isostructural to the borates with a similar molecular formula of $M_{3-n}T_n(BO_3)_2$ (M and T = divalent metal; $n=0$–3).[1d,16] The structure of CZBO shows two-dimensional (2D) $^2[Zn_2(BO_3)_2]_\infty$ double layers consisting of $^1[Zn_2O_6]_\infty$ chains and $[BO_3]$ clusters, which are stacked along the *c* direction and separated by $[CaO_6]$ octahedra (Figure 1b). All the cations in CZBO form only one environment, $[CaO_6]$ octahedron, $[ZnO_4]$ tetrahedron, and $[BO_3]$ unit for Ca, Zn, and B, respectively, stacking along the *c* axis of the unit cell (Tables S2–S4). Two $[ZnO_4]$ tetrahedra form $^1[Zn_2O_6]_\infty$ chains (Figure 1c) via corner-sharing that run parallel to the *c* axis, and the $[BO_3]$ units (Figures 1d, g) further link to all four apical O atoms of $[ZnO_4]$ tetrahedra, with the bridging O atoms of $[BO_3]$ units as linkers to yield the 2D $^2[Zn_2(BO_3)_2]_\infty$ double layers in *ac* plane that are further stacked along the *c* axis to generate the final framework. The $[CaO_6]$ octahedra are in the interlayers (Figures 1b, f). The O(2) and O(3) atoms are in normal three-coordinated environments, whereas four-coordinated O(1) atoms link with two Zn, one B, and one Ca atoms, making CZBO be one of the rare structures of corner-shared $^1[Zn_2O_6]_\infty$ chains with Zn–O–Zn bonding.[1d] Such a crowded coordination environment increases the density of $[BO_3]$ units and hence achieves the enhancement of microscopic hyperpolarizability and polarizability anisotropy.

The structure of CZBO can be regarded as a member of the SBBO-like crystals since they both have similar double-layered configurations (Figures 1a, b, e). Structurally, CZBO has the following benefits when compared with SBBO: i) eliminates the structural instability in SBBO, ii) generates beryllium-free candidates; iii) introduces NLO-active units of $[ZnO_4]$, and iv) improves the interlayer force. First, CZBO shows a stable structural framework, which can be proven by the lower structural convergence factor of CZBO (0.0329) than SBBO (>0.065).[12b] In addition, unlike SBBO,[17] none of the imaginary phonon modes was observed in the phonon spectrum (Figure 2a), indicating the dynamically stable character of CZBO. Second, the substitution of $[BeO_4]$ by $[ZnO_4]$ units generates a beryllium-free NLO crystal that avoids the toxicity issue. Third, CZBO

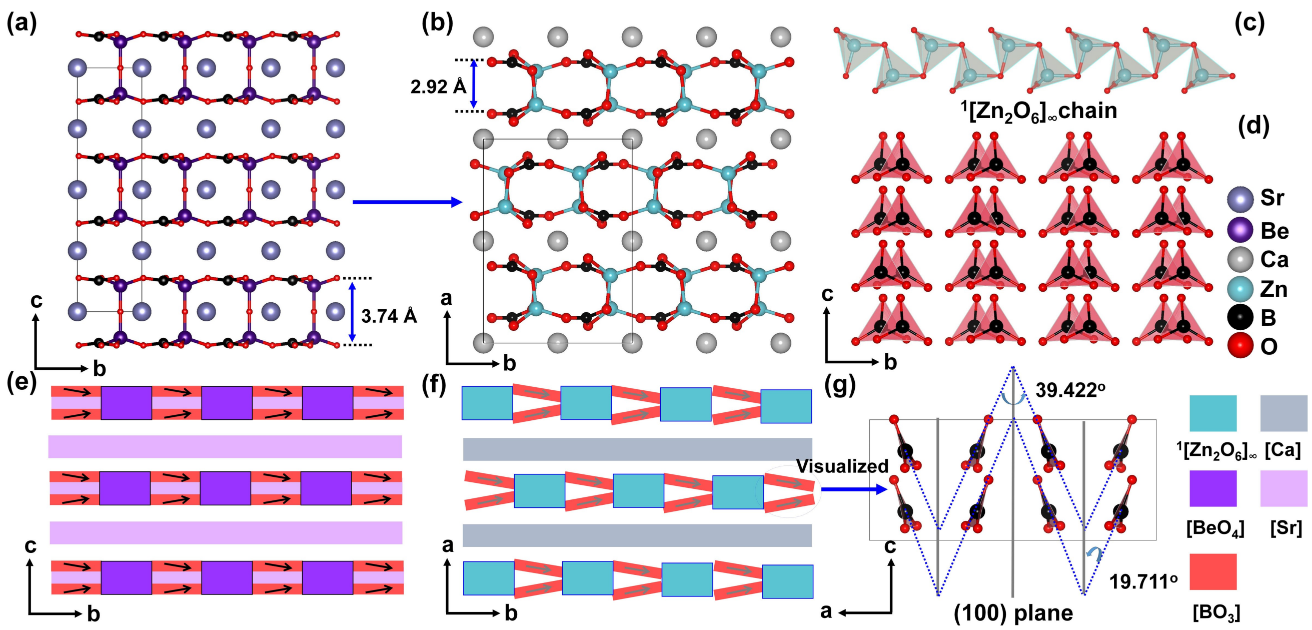

Figure 1. a, b) Structural comparison between $Sr_2Be_2B_2O_7$ and $CaZn_2(BO_3)_2$. c) One-dimensional infinite $^1[Zn_2O_6]_\infty$ chain of corner-sharing $[ZnO_4]$ tetrahedra. d) Optimally aligned arrangement of $[BO_3]$ NLO active units along the *c* axis in $CaZn_2(BO_3)_2$. e, f) Modular description of the arrangement of $[BO_3]$ and $[BeO_4]$/$^1[Zn_2O_6]_\infty$ modules in $Sr_2Be_2B_2O_7$ and $CaZn_2(BO_3)_2$. g) Geometric details in $[BO_3]$ units of $CaZn_2(BO_3)_2$.

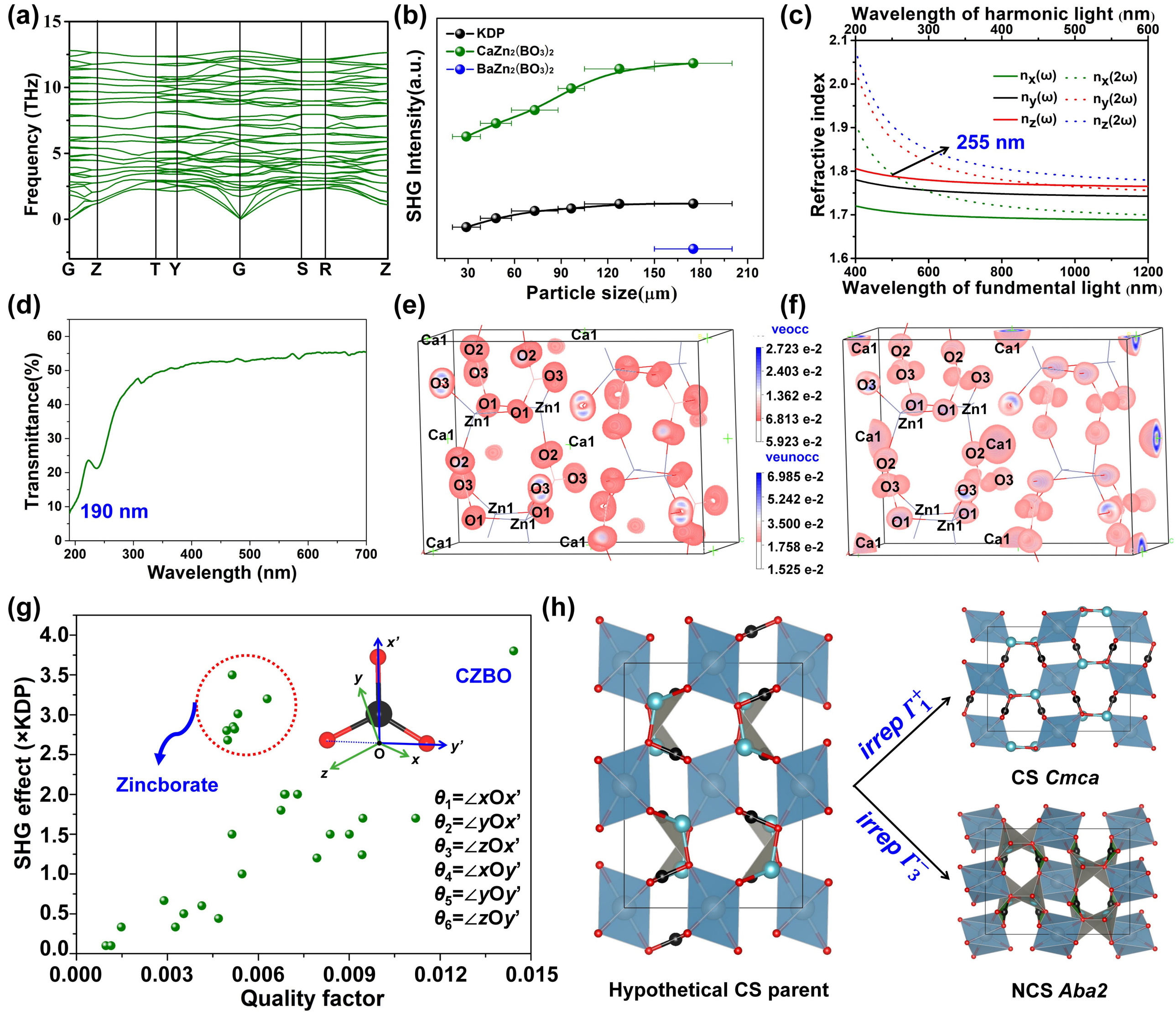

Figure 2. a) Calculated phonon spectrum for $CaZn_2(BO_3)$. b) Relation between the powder SHG intensity and particle size at 1064 nm, and the value of $BaZn_2(BO_3)$ was adapted from ref. [16b]. c) Refractive index dispersion curves for both fundamental and second-harmonic light. The note for this data is available in ref. [18]. d) Transmission spectrum of $CaZn_2(BO_3)_2$ crystal. e, f) The SHG density maps of the occupied (left) and unoccupied (right) orbitals in the virtual electron process. g) Relation between the powder SHG intensity (×KDP) and quality factor ($Q=f(C,\rho)=C\times\rho$), insert gives the established macroscopic (x-y-z) and microscopic (x'-y') coordinates for one $[BO_3]$ group in $CaZn_2(BO_3)_2$ crystal's unit cell when performed the calculation of Q. h) Structural distortion modes decompositions for $CaZn_2(BO_3)_2$.

not only retains the NLO-favorable layered structure and high density of $[BO_3]$ groups but also introduces a extra NLO-active unit of $[ZnO_4]$, which is expected to produce a large SHG response and birefringence. Fourth, layer spacing is reduced from 6.25 Å in KBBF[12a] and 3.74 Å[12] in SBBO to 2.92 Å in CZBO (Figures 1a, b), making it a better growth habit without a strong tendency to layer.

The NLO properties were investigated by both experimental and theoretical approaches since CZBO belongs to the non-centrosymmetric class and all the possible NLO-active units ($[BO_3]$ and $[ZnO_4]$) are in favorable configurations. As a result, CZBO shows a strong PM SHG response of 3.8×KDP@1064 nm (Figure 2b) and high second-order NLO coefficients (cal. $d_{31}=d_{15}=-0.027$ pm V^{-1}, $d_{32}=d_{24}=-1.687$ pm V^{-1}, and $d_{33}=1.486$ pm V^{-1}), for which, the experimental results are consistent with the theoretical ones. In addition, the transmission spectrum measured on a small-sized CZBO crystal indicates that its UV cut off edge is about 190 nm (Figure 2d). It should be noted that such a second-order nonlinearity is the largest among all the available deep-UV transparent borates with only $[BO_3]$ units. More importantly, this NLO response is 38 times higher than that of its non-isomorphic $BaZn_2(BO_3)_2$ parent (0.1×KDP),[16b] indicating that a simple non-isomorphic substitution can achieve a giant nonlinearity enhancement. Meanwhile, the birefringence increased from 0.045 in $BaZn_2(BO_3)_2$ to 0.081 in CZBO, shifting the shortest type **I** SHG PM wavelength from 393 to 255 nm (Figure 2c and Figure S1). When taken together, CZBO crystals have the potential to generate the 266 nm coherent light by the direct fourth harmonic generation (FHG) process once crystals are sufficiently large.[18] The origin of this large nonlinearity and its giant enhancement were analyzed and confirmed by the following measurements:

The SHG-weighted electron density analysis gives the qualitative analysis of individual atoms in CZBO to second-order nonlinearities (Figures 2e,f). In the dominant virtual electron process (virtual electron: virtual hole ≈ 98 % : 2 %), the main contribution in occupied states to the largest tensor of d_{32} originates from the non-bonding O 2p orbitals. Whereas for unoccupied states, both Ca 3d and O 2p orbitals have considerable contributions with a small contribution from B and Zn atoms. This is, however, different from other deep-UV transparent borates where alkali and alkaline-earth metals have small contributions to SHG effects. But, the similar phenomenon is also found in $CaB_5O_7F_3$,[13i] in which Ca also has a considerable contribution. But, all the O(1), O(2), and O(3) atoms in CZBO connect with both B and Zn atoms, which does not allow one to assign these O atoms and hence to state that what are the real NLO-active units in CZBO. Faced with this, we quantified all the groups' dipole moments in the unit cell. As shown in Table S5, $[ZnO_4]$, $[CaO_6]$, and $[BO_3]$ units generate dipole moments of 9.29, 0.85, and 0.47 Debye in the unit cell, respectively. It is important to note that the net dipole moments of all three units are cancelled along the *a* and *b* directions and their vector sums are along the *c* axis, indicating that the contribution of the large nonlinearity in CZBO originates from the superposition effects of $[ZnO_4]$, $[CaO_6]$, and $[BO_3]$ units along the *c* axis.

To further investigate the role of $[BO_3]$ units on the nonlinearity, calculations based on anionic group theory were undertaken.[19] These indicate that the geometrical superposition of microscopic second-order susceptibility tensors of anionic groups is responsible for the nonlinearity. Thus, in the CZBO crystal, the $[BO_3]$ unit was considered. According to the derived formulas presented in the Supporting Information, the second-order NLO coefficient χ_{ijk} is proportional to the density of $[BO_3]$ ($n\,V^{-1}$) units and the structural criterion, $C = f(g,n) = g/n$. Thus, the key is the calculation of g. The CZBO crystal belongs to the $mm2$ point group and has three independent second-order susceptibilities, namely χ_{333}, χ_{131}, and χ_{223} (corresponding to $2\times d_{33}$, $2\times d_{15}$ and $2\times d_{24}$, respectively). According to the equations and the geometric features in two established coordinate systems (see Figure 2g), g_{ijk} is calculated as follows:

$$g_{333} = n[\cos^3\theta_3 - 3\cos\theta_3 cos^2\theta_6] = 8 \times 0.0722$$

$$g_{131} = n[\cos^2\theta_1\cos\theta_3 - 2\cos\theta_1\cos\theta_4\cos\theta_6 - \boldsymbol{cos}^2\theta_4\cos\theta_3] = 8 \times 0.8970$$

$$g_{223} = n[\cos^2\theta_2\cos\theta_3 - 2\cos\theta_2\cos\theta_5\cos\theta_6 - \boldsymbol{cos}^2\theta_5\cos\theta_3] = 8 \times 0.8350$$

Thus, the structural criterion $C = f(g,n)$ is equal to $g/n = \max(g_{ijk})/n = 0.8970$, which indicates that the $[BO_3]$ units mostly add their contributions to the total nonlinearity in the CZBO crystal. In addition, it also shows an extremely large density of $[BO_3]$ units (0.016 Å^{-3}). Considering two aforementioned factors (structural criterion and density of $[BO_3]$ units), the quality factor, $Q = f(C, \rho) = C\times\rho$, was defined, which can provide quantitative analysis of the contribution of $[BO_3]$ units to the total nonlinearity. As expected, CZBO has a large Q of 0.0144 Å^{-3}, which is even larger than that of KBBF and its isomorphic compounds (0.009–0.012 Å^{-3}), more importantly, such a Q value is the largest one among all the available deep-UV transparent beryllium-free borates with $[BO_3]$ units, which is consistent with its large nonlinearity (Figure 2g). Furthermore, the Q value of CZBO is much larger than that of $BaZn_2(BO_3)_2$ (0.001 Å^{-3}), indicating that the giant nonlinearity enhancement of CZBO compared with $BaZn_2(BO_3)_2$ in part arises from the high active density of $[BO_3]$ units.

To further elucidate the superposition effect of the polar distortions on second-order nonlinearity, we also utilized the symmetry-adapted mode decomposition analysis for CZBO,[8f,13d,20] in which the amplitude of each symmetry mode's contribution can be used to understand the atomic displacements that are responsible for symmetry breaking. We performed a symmetry-adapted mode decomposition using the symmetry mode analysis tool of the Bilbao Crystallographic Server,[21] where the pseudosymmetric structures subjected to structural relaxation by performing DFT calculation with lattice constants were fixed at the values in the corresponding experimental structures (see detail in the Supporting Information and Tables S6–S8). We first identified a hypothetical high symmetry structure for CZBO in centrosymmetric *Cmca* (No. 64) (Figure 2h), and free-refined atomic positions by restricting the lattice parameters to our experimentally obtained non-centrosymmetric *Aba*2 (No. 41). Then, two displacive modes were found (Figure 2h): i) The first one is an inversion preserving mode characterized by the irreducible representation (*irrep*) Γ_1^+, which contains fully symmetric displacements of all atoms and thus does not cause symmetry breaking and retains the centrosymmetric *Cmca*. ii) The second *irrep*, Γ_3^-, consists of the following displacements: polar Ca and Zn displacements along the crystallographic *c* axis as well as rotations of O atoms around $[BO_3]$ units (Figure S2). Obviously, all O atoms in CZBO simultaneously link with both Zn and B cation, thus, the inversion symmetry breaking is attributable to the *irrep* Γ_3^- mode owing to the $^2[Zn_2(BO_3)_2]_\infty$ double layers and allows for SHG effects. By superposing the magnitude of these displacements in the *irrep* Γ_3^- mode, the symmetry-adapted mode decomposition is calculated to be close to in KBBF crystal.[13d] Consequently, based on the above four aforementioned analysis approaches, the large SHG effect in CZBO originates from the $^1[Zn_2O_6]_\infty$ polar chains with a large net dipole moment, $[BO_3]$ units with high active density and $[CaO_6]$ polyhedra.

In summary, a new zinc borate with a SBBO-type structure, $CaZn_2(BO_3)_2$ has been reported. This new material eliminates the structural instability and toxicity of raw materials in SBBO. Remarkably, $CaZn_2(BO_3)_2$ shows a balanced property for NLO applications: a large PM SHG reponse (3.8×KDP), a suitable birefringence (0.081@546 nm), a deep-UV cut off edge (< 190 nm), and a short PM wavelength (255 nm). Such a large second-order nonlinearity is the largest among all the available deep-UV transparent borates with $[BO_3]$ units, which is 38 times higher than that of its non-isomorphic $BaZn_2(BO_3)_2$ parent. The combinations of dipole moment calculations, anionic group theory calculations, SHG-weighted electron density analysis, and symmetry-adapted mode decomposition analysis reveal that the large nonlinearity originates from the $^1[Zn_2O_6]_\infty$ polar chains with large net dipole moment, $[BO_3]$ units with high active density and $[CaO_6]$ polyhedra. We believe that the strategy of simple non-isomorphic substitution is a feasible method to achieve the rational design of SBBO-type NLO crystals with enhanced structural stability and nonlinearity, and thus related non-centrosymmetric materials as possible and studies are underway to make them.

Acknowledgements

This work was financially supported the National Key R&D Program of China (2021YFA0717800), Young Elite Scientist Sponsorship Program by CAST (YESS20200068), National Natural Science Foundation of China (52002397, 61835014), the National Science Foundation (NSFDMR1904701), and the West Light Foundation of CAS (2020-XBQNXZ-002).

Conflict of Interest

The authors declare no conflict of interest.

Data Availability Statement

The data that support the findings of this study are available in the supplementary material of this article.

Keywords: Borates · Crystals · Functionalized Units · Nonlinear Optical Materials · Solid-State Chemistry

[1] a) C. T. Chen, T. Sasaki, R. K. Li, Y. C. Wu, Z. S. Lin, Y. Mori, Z. G. Hu, J. Y. Wang, S. Uda, M. Yoshimura, Y. Kaneda, *Nonlinear optical borate crystals: principals and applications*, Wiley-VCH, Weinheim, **2012**; b) T. Sasaki, Y. Mori, M. Yoshimura, Y. K. Yap, T. Kamimura, *Mater. Sci. Eng. R* **2000**, *30*, 1–54; c) T. T. Tran, H. W. Yu, J. M. Rondinelli, K. R. Poeppelmeier, P. S. Halasyamani, *Chem. Mater.* **2016**, *28*, 5238–5258; d) M. Mutailipu, K. R. Poeppelmeier, S. L. Pan, *Chem. Rev.* **2021**, *121*, 1130–1202.

[2] a) N. Taylor, *Laser: the inventor, the Nobel laureate, and the thirty-year patent war*; Simon Schuster, New York. **2007**; b) P. F. Bordui, M. M. Fejer, *Anna. Rev. Mater. Sci.* **1993**, *23*, 321–379.

[3] P. S. Halasyamani, K. R. Poeppelmeier, *Chem. Mater.* **1998**, *10*, 2753–2769.

[4] a) K. M. Ok, *Acc. Chem. Res.* **2016**, *49*, 2774–2785; b) Y. G. Shen, S. G. Zhao, J. H. Luo, *Coord. Chem. Rev.* **2018**, *366*, 1–28; c) J. Chen, C. L. Hu, F. Kong, J. G. Mao, *Acc. Chem. Res.* **2021**, *54*, 2775–2783; d) L. Kang, F. Liang, X. X. Jiang, Z. S. Lin, C. T. Chen, *Acc. Chem. Res.* **2020**, *53*, 209–217.

[5] a) D. H. Lin, M. Luo, C. S. Lin, F. Xu, N. Ye, *J. Am. Chem. Soc.* **2019**, *141*, 3390–3394; b) X. H. Meng, P. F. Gong, C. L. Tang, W. L. Yin, Z. S. Lin, M. J. Xia, *Adv. Opt. Mater.* **2021**, *9*, 2100594.

[6] a) J. Lu, J. N. Yue, L. Xiong, W. K. Zhang, L. Chen, L. M. Wu, *J. Am. Chem. Soc.* **2019**, *141*, 8093–8097; b) M. Mutailipu, Z. H. Yang, S. L. Pan, *Acc. Mater. Res.* **2021**, *2*, 282–291; c) H. P. Wu, B. B. Zhang, H. W. Yu, Z. G. Hu, J. Y. Wang, Y. C. Wu, P. S. Halasyamani, *Angew. Chem. Int. Ed.* **2020**, *59*, 8922–8926; *Angew. Chem.* **2020**, *132*, 9007–9011.

[7] a) I. Chung, M. G. Kanatzidis, *Chem. Mater.* **2014**, *26*, 849–869; b) A. Abudurusuli, J. B. Huang, P. Wang, Z. H. Yang, S. L. Pan, J. J. Li, *Angew. Chem. Int. Ed.* **2021**, *60*, 24131–24136; *Angew. Chem.* **2021**, *133*, 24333–24338; c) Y. Chu, P. Wang, H. Zeng, S. C. Cheng, X. Su, Z. H. Yang, J. J. Li, S. L. Pan, *Chem. Mater.* **2021**, *33*, 6514–6521; d) C. Yang, X. Liu, C. Teng, X. Cheng, Q. Wu, *Mater. Today Phys.* **2021**, *19*, 100432; e) D. J. Mei, W. Z. Cao, N. Z. Wang, X. X. Jiang, J. Zhao, W. K. Wang, J. H. Dang, S. Y. Zhang, Y. D. Wu, P. H. Rao, Z. S. Lin, *Mater. Horiz.* **2021**, *8*, 2330–2334.

[8] a) C. Wu, T. H. Wu, X. X. Jiang, Z. J. Wang, H. Y. Sha, L. Lin, Z. S. Lin, Z. P. Huang, X. F. Long, M. G. Humphrey, C. Zhang, *J. Am. Chem. Soc.* **2021**, *143*, 4138–4142; b) Q. Huang, L. J. Liu, X. Y. Wang, R. K. Li, C. T. Chen, *Inorg. Chem.* **2016**, *55*, 12496–12499; c) G. S. Yang, P. F. Gong, Z. S. Lin, N. Ye, *Chem. Mater.* **2016**, *28*, 9122–9131; d) J. J. Zhou, Y. Q. Liu, H. P. Wu, H. W. Yu, Z. S. Lin, Z. G. Hu, J. Y. Wang, Y. C. Wu, *Angew. Chem. Int. Ed.* **2020**, *59*, 19006–19010; *Angew. Chem.* **2020**, *132*, 19168–19172; e) S. G. Zhao, J. Zhang, S. Q. Zhang, Z. H. Sun, Z. S. Lin, Y. C. Wu, M. H. Hong, J. H. Luo, *Inorg. Chem.* **2014**, *53*, 2521–2527; f) H. W. Yu, H. P. Wu, S. L. Pan, Z. H. Yang, X. L. Hou, X. Su, Q. Jing, K. R. Poeppelmeier, J. M. Rondinelli, *J. Am. Chem. Soc.* **2014**, *136*, 1264–1267.

[9] a) S. G. Jantz, M. Dialer, L. Bayarjargal, B. Winkler, L. Wüllen, F. Pielnhofer, J. Brgoch, R. Weihrich, H. A. Höppe, *Adv. Opt. Mater.* **2018**, *6*, 1800497; b) L. Y. Li, G. B. Li, Y. X. Wang, F. H. Liao, J. H. Lin, *Chem. Mater.* **2005**, *17*, 4174–4180; c) X. Y. Dong, Q. Jing, Y. J. Shi, Z. H. Yang, S. L. Pan, K. R. Poeppelmeier, J. Young, J. M. Rondinelli, *J. Am. Chem. Soc.* **2015**, *137*, 9417–9422; d) G. H. Zou, C. Lin, H. Jo, G. Nam, T. S. You, K. M. Ok, *Angew. Chem. Int. Ed.* **2016**, *55*, 12078–12082; *Angew. Chem.* **2016**, *128*, 12257–12261.

[10] D. Eimerl, *Ferroelectrics* **1987**, *72*, 95–139.

[11] R. K. Li, P. Chen, *Inorg. Chem.* **2010**, *49*, 1561–1565.

[12] a) C. T. Chen, G. L. Wang, X. Y. Wang, Z. Y. Xu, *Appl. Phys. B* **2009**, *97*, 9–25; b) C. T. Chen, Y. B. Wang, B. C. Wu, K. C. Wu, W. L. Zeng, L. H. Yu, *Nature* **1995**, *373*, 322–324.

[13] a) T. T. Tran, N. Z. Koocher, J. M. Rondinelli, P. S. Halasyamani, *Angew. Chem. Int. Ed.* **2017**, *56*, 2969–2973; *Angew. Chem.* **2017**, *129*, 3015–3019; b) S. G. Zhao, L. Kang, Y. G. Shen, X. D. Wang, M. A. Asghar, Z. S. Lin, Y. Y. Xu, S. Y. Zeng, M. C. Hong, J. H. Luo, *J. Am. Chem. Soc.* **2016**, *138*, 2961–2964; c) H. W. Wu, H. P. Yu, S. L. Pan, P. S. Halasyamani, *Inorg. Chem.* **2017**, *56*, 8755–8758; d) H. W. Yu, J. Young, H. P. Wu, W. G. Zhang, J. M. Rondinelli, P. S. Halasyamani, *Adv. Opt. Mater.* **2017**, *5*, 1700840; e) M. Mutailipu, S. L. Pan, *Angew. Chem. Int. Ed.* **2020**, *59*, 20302–20317; *Angew. Chem.* **2020**, *132*, 20480–20496; f) G. Q. Shi, Y. Wang, F. F. Zhang, B. B. Zhang, Z. H. Yang, X. L. Hou, S. L. Pan, K. R. Poeppelmeier, *J. Am. Chem. Soc.* **2017**, *139*, 10645–10648;

g) M. Mutailipu, M. Zhang, B. B. Zhang, Z. H. Yang, S. L. Pan, *Angew. Chem. Int. Ed.* **2018**, *57*, 6095–6099; *Angew. Chem.* **2018**, *130*, 6203–6207; h) M. Luo, F. Liang, Y. X. Song, D. Zhao, F. Xu, N. Ye, Z. S. Lin, *J. Am. Chem. Soc.* **2018**, *140*, 3884–3887; i) Z. Z. Zhang, Y. Wang, B. B. Zhang, Z. H. Yang, S. L. Pan, *Inorg. Chem.* **2018**, *57*, 4820–4823; j) C. C. Jin, H. Zeng, F. Zhang, H. T. Qiu, Z. H. Yang, M. Mutailipu, S. L. Pan, *Chem. Mater.* **2022**, *34*, 440–450; k) C. L. Hu, J. Chen, Z. Fang, R. L. Tang, J. G. Mao, *Chem. Mater.* **2021**, *33*, 4783–4791.

[14] a) R. X. Guo, X. M. Liu, C. Tao, C. C. Tang, M. J. Xia, L. J. Liu, Z. S. Lin, X. Y. Wang, *Dalton Trans.* **2021**, *50*, 2138–2142; b) H. T. Qiu, M. Xia, W. B. Cai, Z. H. Yang, Y. L. Liu, M. Mutailipu, S. L. Pan, *Dalton Trans.* **2021**, *50*, 13216–13219.

[15] Crystal data for CZBO: orthorhombic, *Aba2*, $Z=4$, $a=11.766$ (3) Å, $b=8.5795(16)$ Å, $c=4.9421(10)$ Å, $V=499.36(17)$ Å^3, $\rho_{calc}=3.8437\ \mathrm{g\,cm^{-3}}$, $\mu=10.588\ \mathrm{mm^{-1}}$, $F(000)=552$, crystal size $=0.17\times0.13\times0.09\ \mathrm{mm^3}$; Mo K$\alpha$ ($\lambda=0.71073$); $2\theta=6.926$ to 55.002°, index ranges $=-15\leq h\leq15$, $-10\leq k\leq10$, $-6\leq l\leq6$; reflections collected = 1691, unique reflections (R_{int}) = 516 (0.0738), goodness-of-fit on $F^2=1.014$; R_1/wR_2 [$I\geq2\sigma$ (I)] = 0.0329/0.0572, Flack parameter = 0.03 (6), BASF 0.03, TWIN −1 0 0, 0 −1 0 0, and 0 −1 2. Details data are listed in Tables S1–S4 in Supporting Information and may be obtained from the Cambridge Crystallographic Data Centre and Fachinformationszentrum Karlsruhe Access Structures service on quoting the deposition number 2118293.

[16] a) R. W. Smith, L. J. Koliha, *Mater. Res. Bull.* **1994**, *29*, 1203–1210; b) R. W. Smith, D. A. Keszler, *J. Solid State Chem.* **1992**, *100*, 325–330; c) W. G. Zhang, H. W. Yu, H. P. Wu, P. S. Halasyamani, *Crystals* **2016**, *6*, 68–74; d) D. E. Harrison, F. A. Hummel, *J. Electrochem. Soc.* **1959**, *106*, 24–26; e) X. S. Lv, P. Wang, H. J. Yu, Y. Y. Hu, H. D. Zhang, C. C. Qiu, J. Li, X. P. Wang, B. Liu, Y. Y. Zhang, *Opt. Mater. Express* **2019**, *9*, 3835–3842; f) A. Vegas, F. H. Cano, S. García-Blanco, *Acta Crystallogr. Sect. B* **1975**, *31*, 1416–1419; g) M. Mączka, K. Szymborska-Małek, A. Gagor, A. Majchrowski, *J. Solid State Chem.* **2015**, *225*, 330–334.

[17] X. Y. Meng, X. H. Wen, G. L. Liu, *J. Korean Phys. Soc.* **2008**, *52*, 1277–1280.

[18] Note that the PM wavelength depends on the refractive index dispersion curve (birefringence), and the calculated birefringence is related to band gap and induced scissor operator. Herein, we used two different scissor operators which corresponding to two different experimental band gaps based on the UV-vis-NIR spectrum (with powder polycrystallines, $E_g=5.65$ eV) and transmission spectrum (with a single crystal, $E_g=6.53$ eV). Both results indicate that the shortest type **I** SHG PM wavelength of CZBO crystal is below 266 nm, that is, 255 and 235 nm for above two situations, respectively.

[19] a) C. T. Chen, Y. C. Wu, R. K. Li, *Int. Rev. Phys. Chem.* **1989**, *8*, 65–91; b) N. Ye, Q. X. Chen, B. C. Wu, C. T. Chen, *J. Appl. Phys.* **1998**, *84*, 555–558.

[20] a) H. P. Wu, H. W. Yu, Z. H. Yang, X. L. Hou, X. Su, S. L. Pan, K. R. Poeppelmeier, J. M. Rondinelli, *J. Am. Chem. Soc.* **2013**, *135*, 4215–4218; b) A. Cammarata, W. G. Zhang, P. S. Halasyamani, J. M. Rondinelli, *Chem. Mater.* **2014**, *26*, 5773–5781.

[21] a) E. S. Capillas, G. de la Flor Tasci, D. Orobengoa, J. M. Perez-Mato, M. I. Aroyo, *Z. Kristallogr.* **2011**, *226*, 186–196; b) D. Orobengoa, C. Capillas, M. I. Aroyo, J. M. Perez-Mato, *J. Appl. Crystallogr.* **2009**, *42*, 820–833; c) J. M. Perez-Mato, D. Orobengoa, M. I. Aroyo, *Acta Crystallogr. Sect. A* **2010**, *66*, 558–590.

Manuscript received: February 8, 2022
Accepted manuscript online: March 8, 2022
Version of record online: ■■, ■■

Communications

Nonlinear Optical Materials

M. Mutailipu, F. Li, C. Jin, Z. Yang,
K. R. Poeppelmeier,*
S. Pan* ______ **e202202096**

Strong Nonlinearity Induced by Coaxial Alignment of Polar Chain and Dense $[BO_3]$ Units in $CaZn_2(BO_3)_2$

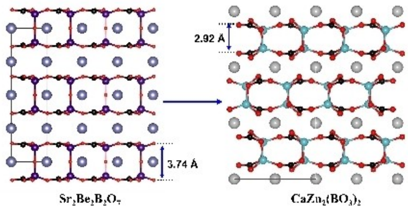

A new beryllium-free borate with double-layered configuration was rationally designed. It shows a large phase-matching second harmonic generation reponse, which is 38 times higher than that of its barium analogue. These findings show the great significance of using tetrahedra to design nonlinear optical crystals and also verify the feasibility of using simple non-isomorphic substitution to induce giant second-order nonlinearity enhancement.

